Synthesis of $Li_{1+\alpha}V_3O_8$ via a Gel Precursor: Part II, from Xerogel to the Anhydrous Material

Matthieu Dubarry,[†] Joël Gaubicher,*[,†] Dominique Guyomard,[†] Nathalie Steunou,[‡] Jacques Livage,[‡] Nicolas Dupré,[§] and Clare P. Grey[§]

Institut des Matériaux Jean Rouxel, 2 rue de la Houssinière, BP 32229, 44322 Nantes Cedex 3, France, Laboratoire de Chimie de la Matière Condensée, Université Pierre et Marie Curie-Paris VI, 4 place Jussieu, 75252 Paris Cedex 05, France, and SUNY, Stony Brook University, New York, New York 11794-3400

Received July 12, 2005. Revised Manuscript Received November 15, 2005

The synthesis of anhydrous $Li_{1+\alpha}V_3O_8$ from its xerogel has been studied by using thermodiffractometry and variable temperature ^{51}V magic-angle spinning NMR spectroscopy. Completion of dehydration leads to a sample characterized by a bimodal grain size distribution, the larger and smaller sized particles coming from the two components of the xerogel (liquid and solid components), respectively. The specific reactions undergone by these two components have been identified: the solid component gradually loses water by undergoing a series of phase transitions involving layered phases with decreasing water concentrations, the hewettite framework being maintained throughout the reaction, whereas in the case of the dried liquid component of the xerogel, the formation of anhydrous $Li_{1+\alpha}V_3O_8$ occurs through the decomposition of lithium vanadates, which is followed by the formation and then progressive dehydration of a hydrated hewettite structure. It is shown that the biphasic nature of the pristine gel precursor has an impact on the electrochemical behavior of anhydrous $Li_{1+\alpha}V_3O_8$.

Introduction

Lithium vanadium oxide, $Li_{1+\alpha}V_3O_8$ ($\alpha = 0.1-0.2$), has been extensively studied over the past 20 years for its attractive electrochemical properties in rechargeable lithium batteries.[1−3] The material consists of $V_3O_8^{3-}$ hewettite[4] layers comprising octahedrally and pentacoordinated vanadium atoms, present in a 2:1 ratio. Intercalation can occur between the layers, the material providing fair energy density and a good capacity retention.[5,6] Two routes have been mainly used to synthesize these oxides, solid-state reactions[2,3,6] and sol−gel synthesis.[5,7] The lithium insertion behavior of $Li_{1+\alpha}V_3O_8$ strongly depends on the firing temperature of the xerogel.[5−7,8] Samples prepared upon heating at 580 °C exhibit a stable capacity of 180 mA·h/g upon cycling,[6] whereas those heated at 350 °C, which can only be prepared using a sol gel route, exhibit a larger initial capacity (300 mA·h/g) that decreases rapidly on cycling.[6,8] Understanding the chemical nature of the gel-like precursor and the chemical processes that lead from the gel-like precipitate to anhydrous $Li_{1+\alpha}V_3O_8$ might suggest new approaches for improving its electrochemical properties.

In a previous paper (Part I),[9] it has been demonstrated that the gel-like precipitate of $Li_{1+\alpha}V_3O_8$ is actually a diphasic mixture, comprising a liquid that contains protonated decavanadic acids and a solid with the formula $Li_{1.1}V_3O_8{\cdot}nH_2O$, consisting of Li^+ ions trapped in porous poorly crystallized hewettite layers. Upon drying at room temperature, the hewettite-like layers of the solid component remain, while the liquid component precipitates, presumably as a mixture of lithiated decavanadates. The decavanadates transform to two hewettite-like compounds upon drying at 90 °C. The dehydration processes of these hydrated $Li_{1.1}V_3O_8{\cdot}nH_2O$ phases that lead to anhydrous $Li_{1.1}V_3O_8$ have never been studied in the literature, although some hydrates synthesized at temperatures below 250 °C have already been investigated in respect to their electrochemical properties.[3,5]

The purpose of this paper is to study the different steps that are involved in the formation of anhydrous $Li_{1+\alpha}V_3O_8$ from its gel-like precursor and to identify and characterize the intermediate phases by using X-ray diffraction (XRD) and ^{51}V magic-angle spinning (MAS) NMR spectroscopy. It will be shown that the diphasic character of the pristine gel-like precursor influences the grain morphology and the

* To whom correspondence should be addressed. E-mail: joel.gaubicher@cnrs-imn.fr. Tel.: 0033 2 40 37 39 32. Fax: 0033 2 40 37 39 95.
† Institut des Matériaux Jean Rouxel.
‡ Université Pierre et Marie Curie-Paris VI.
§ Stony Brook University.

(1) Guyomard, D. In *New Trends in Electrochemical Technology: Energy Storage Systems in Electronics*; Osaka, T.; Matta, D., Eds.; Gordon & Breach: Philadelphia, 2000; Chapter 9, p 253.
(2) Nassau, K.; Murphy, D. W. *J. Non-Cryst. Solids* **1981**, *44*, 297.
(3) Pistoia, G.; Panero, S.; Tocci, M.; Moshtev, R. V.; Manev, V. *Solid State Ionics* **1984**, *13*, 311.
(4) Hillebrand, W. F.; Merwin, H. E.; Wright, F. E. *Proc. Am. Philos. Soc.* **1914**, *53*, 31.
(5) West, K.; Zachau-Christainsen, B.; Skaarup, S.; Saidi, M. Y.; Barker, J.; Olsen, I. I.; Pynenburg, R.; Koksbang, R. *J. Electrochem. Soc.* **1996**, *143*, 820.
(6) Jouanneau, S.; Le Gal La Salle, A.; Verbaere, A.; Guyomard, D.; Deschamps, M.; Lascaud, S. *Solid State Ionics*, in press.
(7) Pistoia, G.; Pasquali, M.; Wang, G.; Li, L. *J. Electrochem. Soc.* **1990**, *137*, 2365.
(8) Jouanneau, S.; Le Gal La Salle, A.; Verbaere, A.; Deschamps, M.; Lascaud, S.; Guyomard, D. *J. Mater. Chem.* **2003**, *13*, 921.
(9) Dubarry, M.; Gaubicher, J.; Guyomard, D.; Durupthy, O.; Steunou, N.; Livage, J.; Dupre, N.; Grey, C. P. *Chem. Mater.* **2005**, *17*, 2276−2283.

10.1021/cm051508+ CCC: $33.50
Published on Web 01/06/2006

electrochemical behavior of anhydrous $Li_{1+\alpha}V_3O_8$ obtained upon firing at 580 °C.

Experimental Section

$Li_{1.1}V_3O_8$ gels have been prepared as described in the literature.[1−3] $LiOH{\cdot}H_2O$ powder was typically reacted with a 2.25 mol·L^{-1} suspension of α-V_2O_5 (Aldrich 99.6%) in distilled water at 50 °C under a N_2 atmosphere for 30 h. Centrifugations of the xerogel were performed at 6400 revolutions/min for 5 min. The liquid part was removed and stored in a Petri dish whereas the solid part was washed with dried ethanol and centrifuged three times. This procedure leads to the separation of the gel into an orange liquid component and a red-brown solid component; these were both dried at room temperature in air. As it will be mentioned in the results section, several hydrates are involved in this study. They have been denoted LVOH*i* where *i* labels them according to their interlayer spacing, irrespective of their water content. The larger the value of *i*, the larger the interlayer distance. Other samples studied in this paper are labeled XG_T, D-LC_T, and D-SC_T for the original xerogel and its dried liquid and solid components (separated by centrifugation), respectively, dried at a temperature *T*.

XRD data were collected ($\lambda_{CuK\alpha}$) with a $\theta/2\theta$ BRUKER D5000 diffractometer with a linear MOXTEK detector, whereas thermodiffractometry was performed on a θ/θ BRUKER D5000 diffractometer. For these latter experiments, the PSD detector mounted on the diffractometer can be fixed at a desired position so that scans of 1000 s were collected over the angular range $2\theta = 6-16°$ following an equilibrium delay of 2000 s at a given temperature. Gels or liquids were cast on a polished glass X-ray holder and dried at room temperature prior to the XRD experiments. Synchrotron experiments were performed using 0.5 mm glass capillaries at the ESRF (Grenoble, France) on the BM01B beam line.

^{51}V MAS NMR experiments were performed on a CMX-360 spectrometer, at an operating frequency of 94.6 MHz corresponding to a field strength of 8.4 T. Spectra were acquired with either a single-pulse sequence or a rotor synchronized ($\pi/12-\tau-\pi/6-\tau-$acq.) echo sequence, where $\tau = 1/\nu_r$ and ν_r is the spinning frequency. $\pi/12$ pulse widths of 1 μs and pulse delays of 0.5 s were used. A Chemagnetics probe equipped with a 3.2 mm rotor was used, with typical spinning frequencies of 15, 20, and 23 kHz. Spectra were acquired at different spinning speeds to determine the frequency of the isotropic resonances. ^{51}V spectra were referenced to a 1 mol·L^{-1} solution of $VOCl_3$ in acetonitrile as an external reference. High-temperature spectra acquisition was achieved using a Chemagnetics variable temperature stack and controller. A lower spinning speed of 15 kHz was used to minimize the temperature gradient between the sample and the thermocouple.

Scanning electron microscopy (SEM) images were obtained from a GEOL 6400 microscope.

Electrochemical measurements were achieved with a MACPILE controller using Swagelok type cells.[4] The composite electrode was coated on Al disks from a mix of 85% of $Li_{1.1}V_3O_8$, 10% of carbon black, and 5% of poly(vinylidene difluoride). EC:DMC (2:1) and $LiPF_6$ was used as the electrolyte. Galvanostatic cyclings were obtained using a current that corresponds to the insertion−desinsertion of 1 Li/2.5 h and 1 Li/5 h per formula unit, respectively, in the 3.7−2 V range. A voltammetry study was also performed in the same potential range at a ±20 mV/h scanning rate. The mass of active material being tested was typically 5 mg/cm^2.

Results and Discussion

XRD of the Dried Samples. XRD patterns of xerogels dried at room temperature and at 90 °C are presented in Figure 1 along with those of their dried liquid and solid components separated by centrifugation. Upon drying at room temperature, the diphasic gel-like precursor of $Li_{1+\alpha}V_3O_8$ consists of a hewettite-like compound $Li_{1+\alpha}V_3O_8{\cdot}3H_2O$ (labeled LVOH3, broad reflections marked by open circles) characterized by an interlayer distance of 10.89 Å and a mixture of lithium decavanadates (LDs; sharp reflections). On the basis of our earlier work and the XRD patterns of D-LC_{25} and D-SC_{25}, the former arises from the solid component while the latter have crystallized from the liquid component.[9] Following drying at 90 °C, LVOH3 partially dehydrates and converts to a second layered phase $Li_{1+\alpha}V_3O_8{\cdot}1.1H_2O$ (LVOH2, marked by *) with a smaller interlayer distance, 10.25 Å, whereas the LDs transform to a similar hewettite like compound (called LVOH1, marked ●). This latter compound has been shown to contain the same water content as LVOH2 but has a smaller interlayer spacing, 7.8 Å.[9] This difference is proposed to arise from different packings of the water molecules and Li ions in the interlayer space.[9]

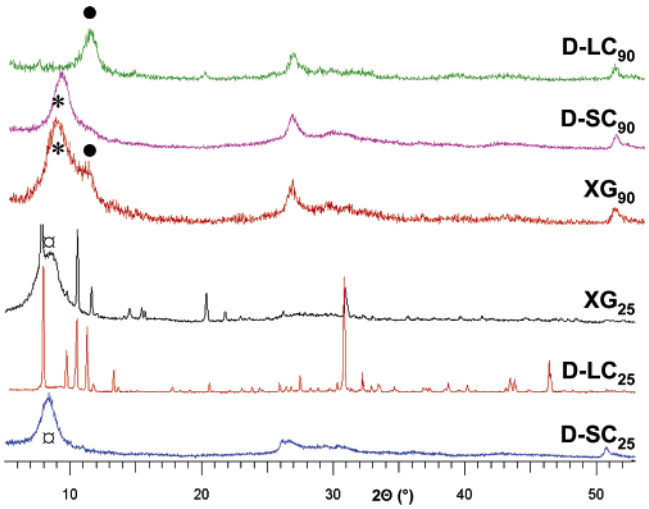

Figure 1. Diffraction patterns of the gel-like precursor and its liquid (D-LC) and solid (D-SC) components dried at room temperature (25 °C) and at 90 °C. The reflections corresponding to the interlayer distance of LVOH1, LVOH2, and LVOH3 are denoted ●, *, and open circles, respectively.

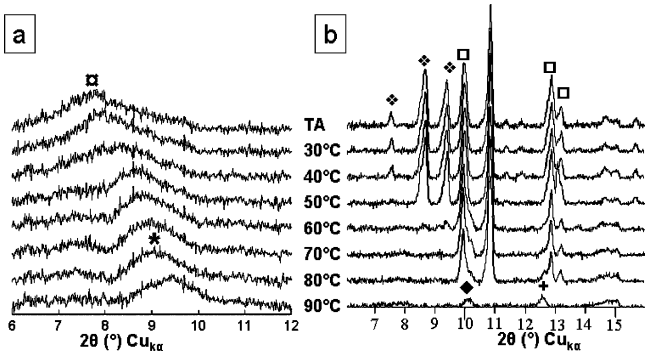

Figure 2. Thermodiffractometry of (a) the solid component of the gel (D-SC) and (b) the liquid component of the gel (D-LC) between room temperature and 90 °C at a 0.2 K/min heating rate. The reflections characteristic of the different phases have been noted as follows: LVOH3 (open circles), LVOH2 (*), $LVOH^3/_2$ (◆), and $LVOH^1/_2$ (+) and, for presumably two lithium decavanadates, LD1 (small diamonds) and LD2 (□).

Thermodiffractometry: Room Temperature to 90 °C. To understand the differences in the phases found following

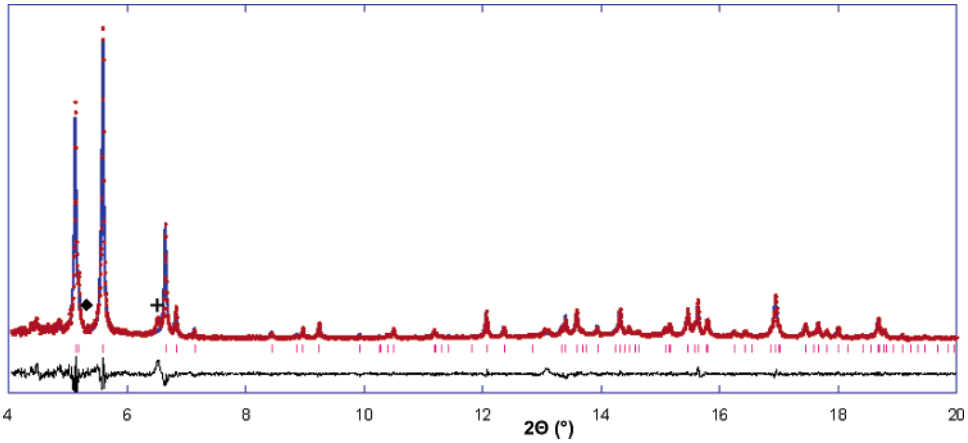

Figure 3. Full pattern matching refinement of the dried liquid component of the gel at 70 °C (D-LC_{70}). Circles correspond to the experimental pattern, and the full line corresponds to the calculated one and to the difference curve. Sticks correspond to calculated Bragg positions.

drying at room temperature and 90 °C and to follow the phase transformations that occur in this range, thermodiffractometry was performed for a small range of 2θ values for both the dried liquid and solid components (D-LC_{25} and D-SC_{25}) of the gel-like precursor (Figure 2). From RT to 90 °C, the solid component of the gel transforms from LVOH3 (open circles) to LVOH2 (*). It starts at 40 °C and is complete by 70 °C (Figure 2a). The evolution of the liquid component is more complex. From 50 to 60 °C, the set of peaks marked by the small diamonds disappears, and a new peak marked by ◆ appears as a shoulder to the reflection at $2\theta = 10°$. Between 80 and 90 °C, the second set of peaks (□) vanishes, and a new peak appears at $2\theta = 12.5°$ (+). From this temperature behavior, it is clear that the liquid component of the gel-like precursor of anhydrous $Li_{1.1}V_3O_8$ must crystallize into two different compounds that are presumably lithium decavanadates on the basis of our earlier work;[9] these phases are denoted LD1 (small diamonds) and LD2 (□).

The reflections due to LD1 and LD2 compounds disappear at 50−60 °C and 80−90 °C, respectively (Figure 2b). The new peaks at $2\theta = 10.1°$ and $2\theta = 12.6°$ at 90 °C were assigned to the (100) reflections of hewettite-like compounds (^{51}V MAS NMR spectra, shown later, confirm that these are hewettite-like phases), respectively $LVOH^3/_2$ ($d = 8.7$ Å (◆)) and $LVOH^1/_2$ ($d = 6.8$ Å (+)). Upon overnight drying at 90 °C, LVOH1 is the only phase that can be observed. $LVOH^3/_2$ and $LVOH^1/_2$ are thus metastable phases that transform to LVOH1 upon annealing. As mentioned in Experimental Section, note that $LVOH^3/_2$ and $LVOH^1/_2$ do not necessarily contain different water contents: indeed a given interlayer spacing does not necessarily correspond to a specific hydration rate because LVOH1 and LVOH2 both contain 1.1 H_2O per formula unit but have quite different interlayer spacings ($d_{LVOH1} = 7.8$ Å and $d_{LVOH2} = 10.25$ Å).[9]

To get a better insight into the nature of LD2, the liquid component was dried at 70 °C for several days. The corresponding diffraction pattern (Figure 3) was collected at the ESRF using synchrotron radiation. The pattern shows some trace of other hydrates, but it mainly comprises LD2. Using Dicvol04 software,[10] LD2 could be indexed in the *Pnnm* space group with $a = 17.62$ Å, $b = 10.32$ Å, and $c =$ 9.22 Å. A subsequent full pattern matching using the winplotr/fullprof package[11] leads to the cell parameters $a =$ 17.6243(3) Å, $b = 10.3259(2)$ Å, and $c = 9.2277(2)$ Å with good reliability factors ($R_{wp} = 8.78$ and $R_{exp} = 7.64$). The structural determination of this phase is underway.

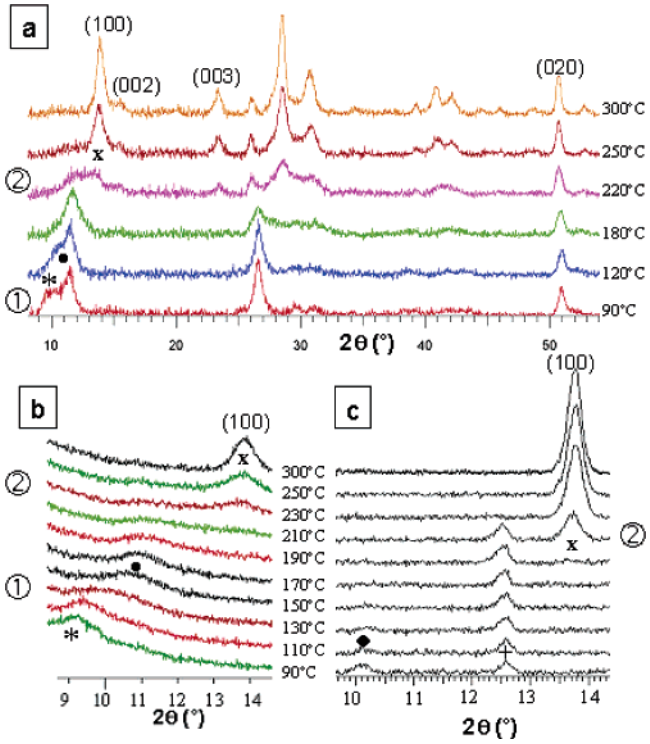

Figure 4. Thermodiffractograms of (a) a dried xerogel at 90 °C (XG_{90}) and (b) its dried solid component (D-SC) and (c) dried liquid component (D-LC). The reflections corresponding to the interlayer distance of LVOH2, LVOH1, $LVOH^3/_2$, $LVOH^1/_2$, and $Li_{1+\alpha}V_3O_8$ are labeled as *, ●, ◆, +, and X, respectively.

Thermodiffractometry: 90−300 °C. On Figure 4a the formation of the crystalline anhydrous $Li_{1.1}V_3O_8$ compound from a xerogel prepared using $[V_2O_5] = 0.75$ mol·L^{-1} and $[LiOH] = 0.55$ mol·L^{-1} dried at 90 °C has been investigated by thermodiffractometry. Two phase transformations are observed. The first one, denoted as ①, occurs between 120 and 180 °C and corresponds to the transformation of LVOH2 (*) into LVOH1 (●). The second one that occurs between

(10) Boultif, A.; Louer, D. *J. Appl. Crystallogr.* **2004**, *37*, 724−731.

(11) Roisnel, T.; Rodriguez, C. *Mater. Sci. Forum* **2001**, *378−381*, 118.

Scheme 1. Schematization of the Thermal Behavior of the Dried Solid (D-SC_{25}) and Liquid (D-LC_{25}) Components of the Gel up to 300 °C as Inferred from XRD

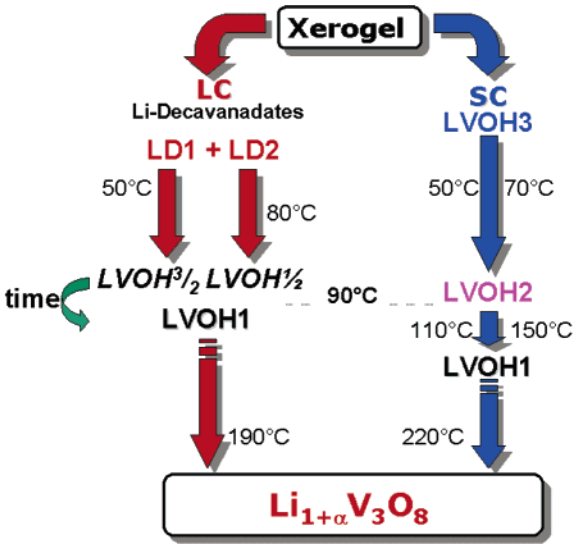

180 and 250 °C, denoted as ②, corresponds to the transformation of LVOH1 into anhydrous $Li_{1.1}V_3O_8$ (×).

To get more precise information concerning the temperature ranges of the phase transformations, thermodiffractometry experiments from 90 to 300 °C were performed for the individual components D-SC_{90} and D-LC_{90} and are shown in Figure 4b,c, respectively. For D-SC, a smooth LVOH2 (*) to LVOH1 (●) transformation occurs from 110 to 150 °C. Given the peak broadening, we cannot rule out the formation of possible intermediate hydrates. Anhydrous $Li_{1.1}V_3O_8$ starts appearing at 220 °C and is pure above 250 °C (the entire pattern from $2\theta = 5$ to 75° is not shown). For D-LC, $LVOH^3/_2$ (◆) disappears between 90 and 130 °C, forming $LVOH^1/_2$ (+). $LVOH^1/_2$ (+) transforms to pure-phase anhydrous $Li_{1.1}V_3O_8$ between 190 and 230 °C. For the sake of clarity results have been summarized in Scheme 1.

The peak widths are much larger for the phases derived from D-SC rather than from D-LC. Single line profile analysis using the integral breadth method with the Holder−Wagner−Landford approximation implemented in WinPlotR[11] was performed on the (100) reflection of the growing anhydrous $Li_{1+\alpha}V_3O_8$ phase. According to this approximation, the Lorentzian component of the pseudo-Voight function used to simulate the peak shape is solely due to size effect, the Gaussian part being associated to microdistortions ($\epsilon = \Delta d/d$). As a consequence, after correction for the instrumental broadening, this method leads to an estimation of the crystallite size (Å) along with a value to the maximal strain (%%). Results reported in Figure 5 show that D-SC $Li_{1.1}V_3O_8$ crystallites are approximately four times smaller than those of D-LC in the direction that is perpendicular to the interlayer space whereas the maximum strain values are lower. We note that an overestimation of the strain effect could lead in turn to an overestimation of the crystallite size. In our case, however, the largest crystallites are those that show the lowest maximum strain.

In light of all of the diffraction results, it appears that only a discrete number of hydrated hewettite-like compounds

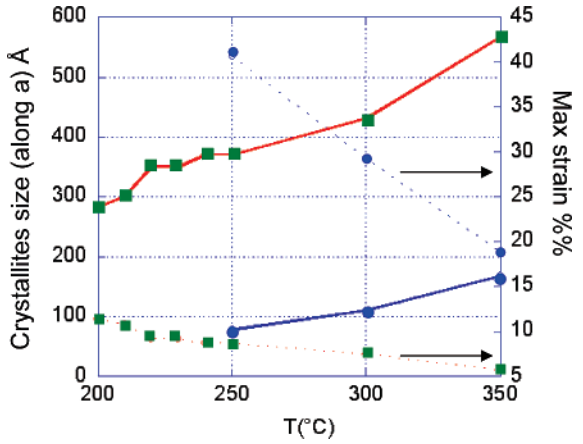

Figure 5. Crystallite size along the *a* direction (solid line) and maximum strain (dashed line) for the dried solid (D-SC; ●) and liquid (D-LC; ■) components of the gel as a function of the temperature.

Table 1. Observed $Li_{1+\alpha}V_3O_8 \cdot nH_2O$ Hewettite-like Compounds, Their Interlayer Spacing According to This Work and Literature,[13−15] and Corresponding Approximate Water Content

	d (Å; this work)	d^{14} (Å)	d^{13} (Å)	d^{15} (Å)	approximate H_2O content (this work, ref 5)
LVOH3	10.89 (open circles)			10.76	3
LVOH2	10.4 (*)				1
$LVOH^7/_4$	9.31	9.04−9.40		9.2	
$LVOH^3/_2$	8.7 (◆)			8.4	?
LVOH1	7.8 (●)	7.71−8.03	7.74	7.55	1
$LVOH^1/_2$	6.8 (+)	7.22			?

exist. This discrete number of hydrates suggests a pillaring effect of water molecules in the interlayer space. In most cases mixtures of these hydrates are actually obtained, which prevents the determination of an accurate water content. For this reason attempts to isolate a desired hydrate were undertaken using controlled hygrometry H_2O/H_2SO_4 atmospheres.[12] Unfortunately, mixtures of hydrates were obtained irrespective of the equilibration time. Nevertheless, a sixth hydrate called $LVOH^7/_4$ ($d = 9.31$ Å) was observed during this study.

Table 1 presents a comparison of the interlayer spacing obtained in this work and in the literature. The *d* spacings observed by us and previous workers are close; LVOH2 has not been observed previously. The broadness of the XRD reflections of these phases is probably responsible for the slight discrepancies observed between the different studies.

^{51}V MAS NMR. Owing to the low crystallinity of the hewettite compounds under investigation, the evolution of the local environments during the formation of crystalline $Li_{1.1}V_3O_8$ has been followed for D-LC_{25} and D-SC_{25}, as a function of temperature, by using ^{51}V MAS NMR spectroscopy.

D-SC_{25}. The evolution of the spectra of D-SC_{25} with temperature is displayed in Figure 6. The spectrum of D-SC_{25} at room temperature contains two sets of resonances at −545

(12) *CRC Handbook of Chemistry and Physics*, 73rd ed.; Lide, D. R.; CRC Press: Boca Raton, FL, 1992−1993.
(13) Manev, V.; Momchilov, A.; Nassalevska, A.; Pistoia, G.; Pasquali, M. *J. Power Sources* **1995**, *54* (2), 501.
(14) Kumagai, N.; Yu, A. *J. Electrochem. Soc.* **1997**, *144* (3), 830.
(15) Pasquali, M.; Pistoia, G.; Manev, V.; Moshtev, R. V. *J. Electrochem. Soc.* **1986**, *133* (12), 2454.

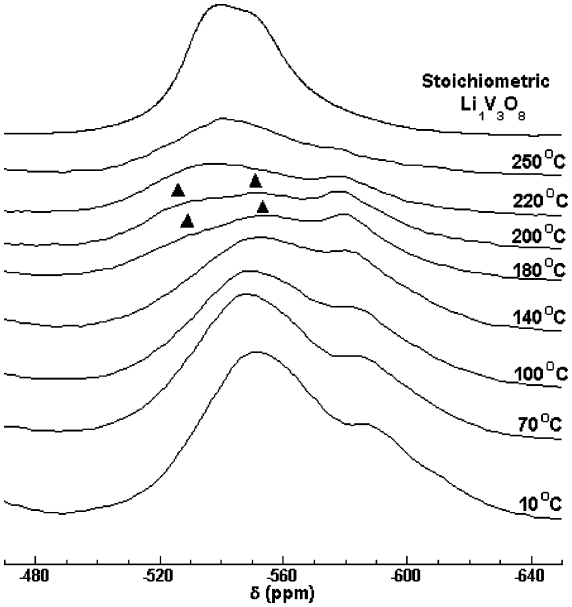

Figure 6. ^{51}V MAS NMR spectra of the dried solid component of the gel (D-SC_{25}) obtained as a function of temperature, acquired at $B_0 = 8.4$ T and $\nu_r = 15$ kHz.

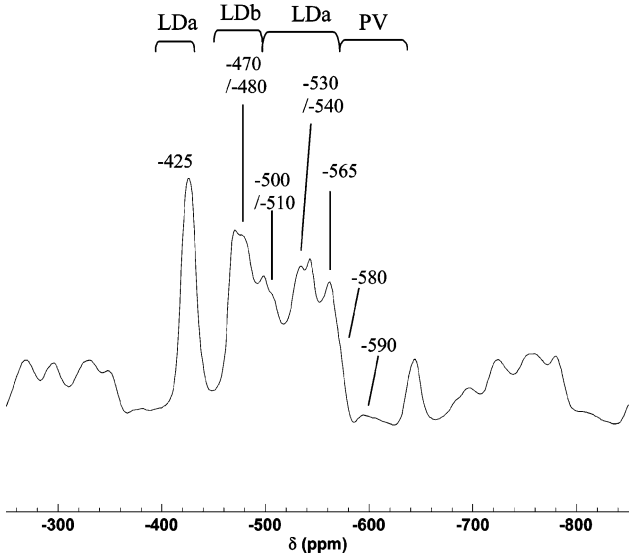

Figure 7. ^{1}V MAS NMR spectra showing the isotropic resonances of the dried liquid component of the gel (D-LC_{25}), acquired at $B_0 = 8.4$ T and $\nu_r = 20$ kHz. All the remaining peaks arise from spinning sidebands.

and −580 ppm (as shown in Part I),[9] indicating that there are at least two different local environments for vanadium. These resonances are present in an approximately 2:1 ratio, respectively,[9] consistent with a hewettite type structure comprising corrugated vanadium oxide layers similar to those found in anhydrous $Li_{1+\alpha}V_3O_8$, with two octahedrally coordinated (−545 ppm) ions and one pentacoordinated vanadium (−580 ppm) ion. The shifts are in the same range as those seen in $NaV_3O_8 \cdot H_2O$, which also contains hewettite layers (−548 ppm (five-coordinate) and −535 ppm (octahedral V)).[16]

Three intermediate hydrated phases (LVOH1, 2, and 3) were identified by XRD in the investigated temperature range (Table 1). LVOH1 (150−220 °C) and LVOH2 (70−110 °C) both contain one interlayer water molecule per formula unit at 90 °C but have different interlayer spacings, while LVOH3 (room temperature to 70 °C) contains the same vanadium oxide layers but has two additional water molecules per formula unit at room temperature. Thus, we expect the vanadium local environments within these three compounds to be similar. Indeed, no dramatic changes are observed in the spectra as the temperature increases, consistent with the presence of very similar vanadium local environments in the D-SC sample throughout the heating process. The severe overlap of the different broad resonances do not allow an accurate simulation of the chemical shift anisotropy and quadrupolar coupling parameters, which might have provided further information concerning the coordination environments of the vanadium sites.

A slight change in the line shape is detected by a careful examination of the spectra obtained between 70 and 100 °C and is ascribed, by comparison with data from XRD experiments, to the formation of LVOH2. A larger change is seen between 140 and 180 °C, ascribed to the formation of LVOH1. Two resonances are resolved at approximately −535 and −555 ppm (marked by black triangles) at 180 °C, in addition to the resonance due to the pentacoordinated site (−580 ppm). These can be attributed to vanadium in two slightly different octahedral environments. The larger changes seen in this temperature range are ascribed to the loss of the structural water on going from LVOH2 and LVOH1 and the consequent rearrangement of the water layers and Li^+ ions. Li^+ ions are likely more strongly bound to the hewettite framework following the partial dehydration.

Above 220 °C, a spectrum that resembles that of crystalline $Li_{1+\alpha}V_3O_8$ is observed, although noticeable increases in line width of the overlapping resonances result in a more featureless line shape for the sample derived from D-SC. The resonance assigned to pentacoordinated vanadium (−580 ppm) broadens and appears as a shoulder of the resonances ascribed to octahedral vanadium, as was seen in the spectrum of the crystalline $Li_{1+\alpha}V_3O_8$. The resonances have also shifted toward lower frequencies with respect to spectra obtained at low temperature and are now at similar frequencies to those found for the crystalline $Li_{1+\alpha}V_3O_8$.[17]

The increased line width is attributed to the poorer crystallinity of the D-SC derived $Li_{1.1}V_3O_8$ sample, caused by the lower synthesis temperature. No change is observed in the ^{51}V resonances when the samples are cooled to room temperature.

D-LC_{25}. The spectrum of D-LC_{25}, previously presented in the Part I,[9] is shown again in Figure 7 in view of the complexity of this spectrum, which contains 10 different isotropic resonances. Our previous study (Part I)[9] indicated that D-LC_{25} consists predominantly of decavanadic acids and polyvanadic species, as opposed to a single V_2O_5-type phase: the presence of decavanadates is characterized by resonances at −425, −500, −510, −530, and −542 ppm (labeled LDa on Figure 7).[18,19] Shifts of −470 and −480

(16) Durupthy, O.; Steunou, N.; Coradin, T.; Maquet, J.; Bonhomme, C.; Livage, J. *J. Mater. Chem.* **2005**, *15* (10), 1090.

(17) Dupre, N.; Gaubicher, J.; Guyomard, D.; Grey, C. P. *Chem. Mater.* **2004**, *16* (14), 2725.

(18) Donnell, S. E. O.; Pope, M. T.; Dalton, J. C. S. **1976**, 2290.

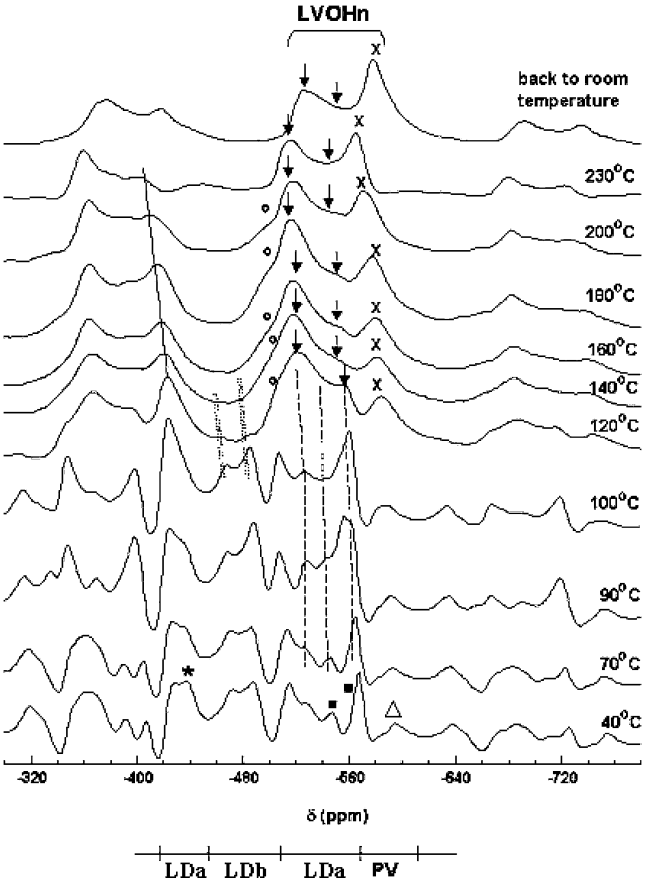

Figure 8. An enlargement of ^{51}V MAS NMR spectra of the dried liquid component of the gel (D-LC) obtained as a function of temperature with $B_0 = 8.4$ T and $\nu_r = 15$ kHz showing the isotropic resonances and the first set of spinning sidebands. The scale shown below the chemical shift axis gives the chemical shift range of the different vanadium species observed at room temperature, as shown in Figure 7.

ppm (labeled LDb) were assigned to the local environment deviating slightly from that of decavanadates or precipitates formed by the Li^+ ions and the polyvanadate species. Resonances at −565 and −590 ppm (labeled PV) are usually attributed to polyvanadate ions or to pentacoordinated vanadium environments found in gels of V_2O_5.[20] The resonance at −565 ppm contains a shoulder at higher frequencies at approximately −580 ppm, which is assigned to similar local vanadium environments.

Spectra of the same sample obtained from a second set of experiments using a slightly lower spinning speed of 15 kHz for D-LC_{25}, as a function of temperature, are shown in Figure 8. The first spectrum was obtained at 40 °C and is closely related to that of D-LC_{25}. The same resonances are observed; however, the slower spinning speed results in overlap between the higher and the lower frequency resonances and changes in relative intensities of the isotropic resonances. For example, the signal at −590 ppm (marked by an open triangle) is associated with a more intense sideband at −438 ppm (marked by *), and the resonance at −565 ppm is more intense.

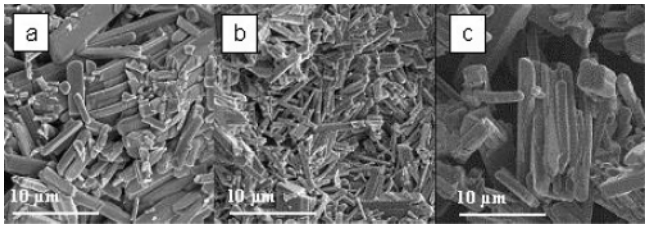

Figure 9. SEM images showing the morphology of (a) the xerogel XG_{580}, (b) the dried solid component (D-SC_{580}), and (c) the dried liquid component (D-LC_{580}) heated at 580 °C for 10 h.

No significant change is observed from room temperature to 100 °C, apart from an overall growth in intensity of the resonances between −510 and −560 ppm (dashed lines). The thermodiffractometry analysis indicates the formation of a hydrated hewettite phase in this temperature range, namely, $LVOH^3/_2$. Resonances at −530 to −590 ppm were observed in Figure 7a of Part I[9] for the hydrated hewettite phases. Thus, the observed progressive increase in intensity in this frequency range may reflect the start of the formation of the vanadium octahedral environments found in a hewettite type compound.

More noticeable changes occur between 100 and 120 °C, the resonances at −470 and −480 ppm, marked by double dashed lines, vanishing to the benefit of resonances in the frequency range of those attributed to vanadium in hewettite phases (−520, −555 (octahedral vanadium, marked by arrows) and −585 ppm (pentacoordinated, marked by an X)). Thus, this change is associated with the reaction of the remaining lithiated decavanadic acids to form a hydrated hewettite compound, probably $LVOH^1/_2$, as suggested from XRD studies in this temperature range. Note that the signal observed at −590 ppm at low temperature and in V_2O_5 gels is also related to pentacoordinated vanadium, as inferred from its chemical shift, but most likely in a different phase because the hewettite structure is not formed at low temperature in the liquid component.

The signal at −426 ppm, assigned to a decavanadate, also disappears in this temperature range, the sidebands of the −585 ppm hewettite resonance now being observed in this frequency range (indicated by the solid line). Additional experiments performed between 70 and 130 °C at the higher spinning speed of 23 kHz confirmed that the resonance at −426 ppm disappears between 100 and 110 °C, consistent with the transformation of decavanadic acid into a hewettit-like structure above 100 °C.

The line shape and numbers of overlapping peaks at approximately −520 ppm, due to octahedral vanadium ions in the hewettite structure, gradually change between 140 and 230 °C. The environments giving rise to highest frequency signals (marked by a circle) disappear above 200 °C. XRD experiments in this temperature range indicated the presence of $LVOH^1/_2$ and LVOH1. Therefore, these resonances are assigned to vanadium in the octahedral site in one or both of these phases. By further increasing the temperature, the resonances rising from vanadium in the octahedral sites (−520 and −555 ppm, marked by arrows) and pentacoor-

(19) Harrison, A. T.; Howarth, O. W.; *J. Chem. Soc., Dalton Trans.* **1985**, 1173.
(20) Fontenot, C. J.; Wiench, J. W.; Schrader, G. L.; Pruski, M. *J. Am. Chem. Soc.* **2002**, *124*, 8435.
(21) Bourgeon, N. Ph. D. Thesis, IMN, Nantes, France, 2003.
(22) Gaubicher, J.; Baethz, C.; Petit, P. E.; Bourgeon, N.; Guyomard, D. *Electrochim. Acta*, submitted.

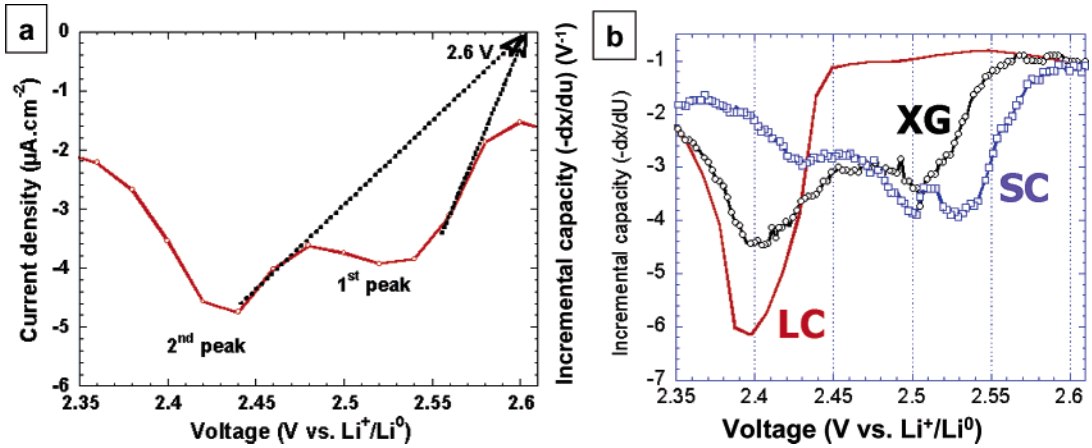

Figure 10. (a) Voltammetric investigation of the structural phase transformation at 2.6 V on the first discharge (−20 mV/h) of $Li_{1.1}V_3O_8$ prepared at 580 °C. Two peaks are observed with a similar equilibrium potential upon 24 h. (b) Incremental capacity curves from galvanostatic cycling (1 Li/2.5 h) of anhydrous $Li_{1.1}V_3O_8$ obtained from the xerogel (XG) and the dried solid (D-SC) and liquid (D-LC) components fired for 10 h at 580 °C.

dinated vanadium (−585 ppm marked by an X) shift to −515, −540, and −565 ppm respectively, at 230 °C. They correspond clearly to the resonances observed at −525, −545, and −580 ppm in the spectrum of the sample cooled back to room temperature and to the resonances seen at −535, −550, and −575 ppm in the spectrum of the stoichiometric $Li_{1.0}V_3O_8$ (cf. Part I),[9] supporting their assignment to environments similar to those found in $Li_{1+\alpha}V_3O_8$.

Noticeable differences between the line shapes and the chemical shifts of the isotropic resonances of D-SC and D-LC at high temperature are observed, although materials with the same stoichiometry and structure are believed to be present. For example, the resonance ascribed to the pentacoordinated vanadium (at approximately −580 ppm) appears to be much sharper and intense in the D-LC spectrum than in that of D-SC. The possibility that the differences may arise from incomplete dehydration of the hewettite phases at 230 °C in the NMR rotor was investigated by heating a D-LC sample at 250 °C for 24 h, in an oven, ensuring complete dehydration of the final $Li_{1+\alpha}V_3O_8$ product. The corresponding NMR spectrum was similar to that obtained in situ at 230 °C. The differences between the $Li_{1+\alpha}V_3O_8$ spectra of samples derived from D-SC and those of samples derived from D-LC must arise from differences in crystallinity and possibly small changes in Li^+ content and/or Li^+ arrangements within the $V_3O_8^-$ layers. Slight differences in Li^+ content and, therefore, the vanadium oxidation state may be responsible for the temperature dependence of the ^{51}V spectrum in the case of the D-LC sample but not in the D-SC sample.

SEM Studies. Upon heating at 580 °C for 10 h, both D-LC or D-SC give rise to pure $Li_{1.1}V_3O_8$, as shown by XRD, but the samples have very different grain sizes (Figure 9). LC leads to large rodlike particles (Figure 9c), about 10 times longer and 4 times thicker than those obtained from D-SC (Figure 9b; 10 μm vs 3 μm). A mixture of small and large particles is observed for the $Li_{1.1}V_3O_8$ powder obtained upon heating XG_{90} at 580 °C (Figure 9a). A recent study[21] showed that the rate of growth along the three axes is well established, resulting in crystallites of dimensions ($3a \times 16b \times 5c$) irrespective of their size (and thus of the temperature at which they have been obtained). As a consequence the bimodal grain size distribution in the sample derived from the xerogel must be due to the differences in crystallite size that arise from the D-SC and D-LC components of the xerogel (Figure 9). We believe that this bimodal character of the $Li_{1.1}V_3O_8$ grain size should always be observed upon firing any gel precursor of $Li_{1+\alpha}V_3O_8$ above 250 °C, because it is intrinsic to the diphasic character of the $Li_{1.1}V_3O_8$ gel.

Electrochemistry. Studies were performed to explore the effect of particle size on the electrochemical behavior. It has been shown[22] that Li insertion in $Li_{1.1}V_3O_8$ prepared at 580 °C at 2.6 V is associated with a structural phase transformation whose kinetics is controlled by that of a nucleation and growth process. On cycling $Li_{1.1}V_3O_8$ in practical conditions, it has been shown that this 2.6 V process splits into two peaks, labeled first peak and second peak (Figure 10a). Both processes commence at close to 2.6 V as seen from the linear extrapolation of the ascending part of the $|J|$ versus V curve on the V axis (see the dashed lines in Figure 10a). Indeed, if the current is stopped at the potential that corresponds to the maximum of these peaks, the batteries equilibrate in both cases to the same OCV (open circuit voltage) value of 2.615 V. Accordingly these two peaks were proposed to correspond to the same phase transformation but would be associated with different kinetics.

Figure 10b shows the incremental capacity curves obtained from galvanostatic cycling of $Li_{1.1}V_3O_8$ samples obtained from XG, D-SC, and D-LC upon firing at 580 °C for 10 h. In the case of XG_{580} two peaks F1 and F2 are observed whereas both SC_{580} and LC_{580} derived $Li_{1.1}V_3O_8$ contain only one peak: the first peak, related to highest kinetics, is observed for SC−$Li_{1.1}V_3O_8$ (small grains) whereas the second peak associated to lowest kinetics appears for LC−$Li_{1.1}V_3O_8$ (large grains). These results demonstrate the effect of the bimodal grain size distribution of the material.

Conclusion

The transformation of the $Li_{1+\alpha}V_3O_8 \cdot nH_2O$ xerogel to anhydrous $Li_{1+\alpha}V_3O_8$ has been investigated by using thermodiffractometry and variable temperature ^{51}V MAS NMR spectroscopy. The starting biphasic xerogel shows reactions that are specific to the solid and liquid initial components

of the gel. The solid component, the hewettite $Li_{1+\alpha}V_3O_8 \cdot 3H_2O$, smoothly dehydrates to form $Li_{1+\alpha}V_3O_8$ whereas the liquid component undergoes two additional reactions that correspond to the transformation of two lithium vanadates to hewettite-like hydrates. Both components lead to anhydrous samples with a monomodal grain size distribution, the size of the crystallites and grains being roughly four times larger in the case of the liquid-based sample. The small size of the $Li_{1+\alpha}V_3O_8$ derived from the solid component is ascribed to the formation of the hewettite layers at room temperature. The decavanadates and polyvanadates that crystallize from the liquid component transform to a hewettite phase only slightly above room temperature, and so the larger crystallite size is most likely due to the larger crystallite sizes of the deca/polyvanadates that crystallize from the liquid. A bimodal grain size distribution is seen in $Li_{1+\alpha}V_3O_8$ prepared from its xerogel, the two sets of differently sized particles being derived from the two components present originally in the xerogel. The bimodal grain size distribution is associated with the different kinetics for the Li insertion reaction that occurs in $Li_{1.1}V_3O_8$ at 2.6 V. Ongoing work is now devoted to the role of each component of the precursor on the electrochemical behavior of anhydrous $Li_{1+\alpha}V_3O_8$ prepared at 350 °C as it is known to present a very high initial capacity that decreases on cycling.[6,8]

Acknowledgment. This work was done with financial support of CNRS and region Pays de la Loire. C.P.G. and N.D. thanks the NSF (Grant DMR021135).

CM051508+